

Accurate Estimation of Drawbar Pull of Wheeled Mobile Robots Traversing Sandy Terrain Using Built-in Force Sensor Array Wheel

Keiji Nagatani, Ayako Ikeda, Keisuke Sato and Kazuya Yoshida

Abstract—The wheels of planetary rovers that are used in space explorations sometimes slip or lose contact with the ground while traversing a sandy terrain. In order to estimate the behavior of these rovers moving on loose soil, it is very important to accurately estimate the drawbar pull of their wheels. Some wheel-soil interaction models based on terramechanics have been proposed for the estimation of the normal stress distribution and drawbar pull of such rovers. However, our experimental results (normal stress distributions are directly measured using a pressure sensor array, which is attached to the wheels of a rover) show that the distribution range of normal stress for small wheeled rovers obtained using the proposed method is considerably smaller than that obtained by using conventional method. Consequently, the drawbar pull estimated using conventional methods is inaccurate. Therefore, in this study, the normal stress distribution is directly measured using pressure sensors in order to estimate drawbar pull accurately. From the data obtained using the sensors, a soil parameter, which is generally very difficult to measure, is estimated. Then, the drawbar pull is estimated using this parameter. The drawbar pull estimated by using the proposed method is more accurate than that estimated using conventional methods. In this study, we propose a new method for the estimation of drawbar pull and also validate this method.

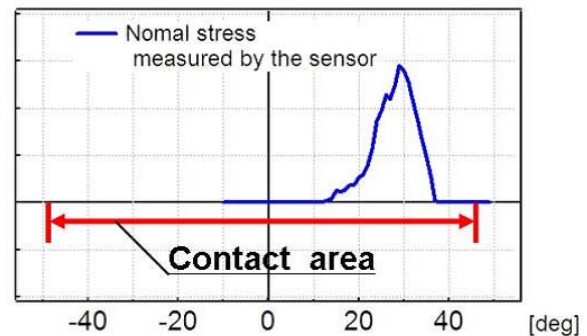


Fig. 1. Obtained range of normal stress distribution

I. INTRODUCTION

Mobile robots (rovers) are indispensable for space exploration missions. The success of the “Mars Exploration Rover (MER) Mission” (JPL/NASA) has shown that mobile robots form an integral part of space missions [1]. The wheels of planetary rovers sometimes slip on the surfaces of Mars or Moon, since their surfaces are covered with fine-grained sand. Wheel slippage may prevent the smooth navigation of rovers. In the worst case, wheels may get stuck in loose soil. In fact, “Opportunity,” which is one of the rovers of the MER mission, had got stuck in a small sand dune in May 2005, thereby jeopardizing the mission. In order to prevent the wheels of rovers from slipping or getting stuck in soil, it is very important to estimate the behavior of rovers well in advance.

The problem mentioned above can be solved by applying the concepts of terramechanics, which is a study of the mechanics of wheel-soil interaction. A wheel-soil interaction model has been proposed by M.G.Bekker, a pioneer in the field of terramechanics[2] [3]. This model has been modified and applied to various types of soils by J.Wong and A.R.Reece [4]. Recently, these models have been applied to the motion analysis of planetary rovers [5] [6].

Keiji Nagatani and Kazuya Yoshida are with Faculty of the Graduate School of Engineering, Tohoku University, 6-6-01, Aramaki aza Aoba, Sendai 980-8579, JAPAN keiji@ieee.org

The wheel-soil interaction model is based on the assumption of ideal conditions, homogeneous soil and flat terrain. Moreover, many unknown soil parameters such as the shear deformation that depends on the slip ratio of wheel, are used in these models. Therefore, in the real environment, it is difficult to estimate the accurate behavior of rovers using unknown parameters. Some studies are underway to determine these unknown parameters[7] [8] [9]. However, in these studies, some external device embedded in the target environment is required to measure some of these parameters or phenomena. Therefore, it is difficult to estimate the behavior estimation of rovers in real outdoor environments by using the methods developed in these studies.

Our objective is to estimate the behavior of rovers online in real environments with only mounted sensors on it. For this purpose, it is important to accurately estimate the drawbar pull of wheels. According to terramechanics, information regarding normal stress and shear stress is required to estimate the drawbar pull of a wheel.

In order to determine the normal stress on a wheel using only mounted sensors on the rover, we have developed a built-in force sensor array (BFSA) wheel. Measuring the normal stress directly eliminates the need for measuring some parameters in advance. During the initial testing of

the wheel, we observed a very interesting phenomenon; the measured area of normal stress was found to be considerably smaller than the contact area between the wheel and the ground in typical cases, as shown in Figure 1. In fact, the phenomenon depends on the size of wheels, the vertical load and soil properties. Although we have used loose sand (Toyoura sand) and a 12 kg four-wheeled mobile robot, the normal stress distribution $\sigma(\theta)$ is very narrow and the stress is distributed on the front section of the contact area between the wheel and the ground. We believed that the normal stress is assumed to be widely distributed in the wheel-soil contact area, and the distribution is estimated by visually observing wheel sinkage. One of the reasons for the phenomenon may come from the size of the wheels. The radius of our wheel is 0.055 m. Anyway, the BFSA wheel is very important to accurately estimate soil parameters for estimating the drawbar pull in advance.

The slip ratio s is another important parameter used to estimate the drawbar pull because it is closely to the shear stress τ . A motion measurement system using a telecentric optics has been developed in our laboratory to estimate s online; this system is based on a visual odometry technique and is used to measure the robot velocity without using external devices embedded in the target environment. The feature of the system is that telecentric optics keeps the same field of view with a change of distance between the camera and the ground, so that the visual odometry is applicable on loose soil. An overview of this system is presented in [10], and a detailed explanation of this system will be reported in another paper.

By using the BFSA wheel and motion measurement system using a telecentric optics, we have developed an online estimation technique for the estimation of a drawbar pull.

This paper is organized as follows. The drawbar pull model based on terramechanics is introduced in Section 2. The development of the BFSA wheel is reported in Section 3, and the measurement experiments carried out to determine $\sigma(\theta)$ using the BFSA-wheel are described in Section 4. A method for the estimation of soil parameters is proposed in Section 5. A method used for the online estimation of drawbar pull using these parameters is described in Section 6.

II. ESTIMATION OF DRAWBAR PULL OF WHEEL ROTATING ON LOOSE SOIL BASED ON TERRAMECHANICS

Bekker's normal stress distribution model is used to estimate the drawbar pull of a wheel rotating on loose soil [3]. In this section, the drawbar pull model based on terramechanics is given.

A. Wheel-soil interaction model

Fig. 2 shows a schematic diagram of $\sigma(\theta)$ under a wheel rotating on loose soil. According to terramechanics, this wheel is subjected to the normal stress σ and a shear stress τ . In Fig. 2, θ_f , θ_r , and θ_m denote the entry angle, the exit angle, and the angle at which σ is maximum, respectively. Note that the vertical direction is $\theta_0 = 0$.

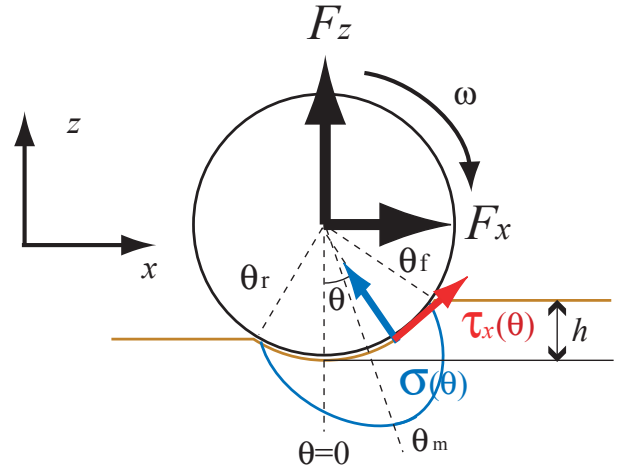


Fig. 2. Wheel-soil interaction model for loose soil

The drawbar pull F_x , given by Equation (1), is calculated by integrating the horizontal components of σ and τ in the contact area. Moreover, the vertical force F_z , given by Equation (2), is calculated by the integrating the vertical components of σ and τ in the contact area. Here, r and b denote the radius and width of the wheel, respectively.

$$F_x = rb \int_{\theta_r}^{\theta_f} \{\tau_x(\theta) \cos \theta - \sigma(\theta) \sin \theta\} d\theta, \quad (1)$$

$$F_z = rb \int_{\theta_r}^{\theta_f} \{\tau_x(\theta) \sin \theta + \sigma(\theta) \cos \theta\} d\theta. \quad (2)$$

B. Bekker's normal stress distribution model

On the basis of Bekker's model, $\sigma(\theta)$ is split into two components at θ_m , as follows:

$$\sigma_f(\theta) = \left(\frac{k_c}{b} + k_\phi \right) [r(\cos \theta - \cos \theta_f)]^n, \quad (3)$$

$$\sigma_r(\theta) = \left(\frac{k_c}{b} + k_\phi \right) \left[r \left(\cos \left\{ \theta_f - \frac{\theta - \theta_r}{\theta_m - \theta_r} (\theta_f - \theta_m) \right\} - \cos \theta_f \right) \right]^n, \quad (4)$$

where k_c and k_ϕ denote pressure-sinkage modulus, n denotes the sinkage exponent that is an inherent parameter of soil, and θ_f , θ_m , and θ_r are the state quantities of the wheel that change according to the wheel rotation. Conventionally, these values are estimated from the sinkage of the wheel, h , as follows:

$$\theta_f = \cos^{-1} \left(1 - \frac{h}{r} \right), \quad (5)$$

$$\theta_r = \cos^{-1} \left(1 - \frac{\kappa h}{r} \right), \quad (6)$$

$$\theta_m = (a_0 + a_1 s) \theta_f, \quad (7)$$

where the parameters a_0 and a_1 are empirical parameters that depend on the target soil. s is defined by the following equation:

$$s = 1 - v_x/r\omega \quad (8)$$

where v_x and ω denote the translational velocity of the robot and the rotational velocity of the wheel, respectively.

C. Bekker's shear stress distribution model

The expression for the shear stress distribution $\tau_x(\theta)$ under a wheel was formulated by Janosi and Hamamoto [11], is given as follows:

$$\tau_x(\theta) = (c + \sigma(\theta) \tan \phi)[1 - e^{-j_x(\theta)/k_x}], \quad (9)$$

where the parameter j_x denotes soil deformation and is a function of θ [12]:

$$j_x(\theta) = r[\theta_f - \theta - (1 - s)(\sin \theta_f - \sin \theta)] \quad (10)$$

where c and ϕ denote the cohesion stress and internal friction angle of soil, respectively. These parameters are inherent parameters of the target soil and are constant. k_x denotes the shear deformation modulus.

D. Essential parameters for estimation of F_x

Using the above-mentioned equations, a drawbar pull can be estimated by measuring s , h , and some assumed parameters, shown in sections II-A – II-C. However, the actual area under normal stress area measured by using the BFSAs-wheel in our initial tests is not equal to the contact area estimated from h . This implies that Equations (5) and (6) cannot be used under the current experimental conditions. Moreover, even if θ_f and θ_r are estimated correctly, it is difficult to estimate θ_m because a_0 and a_1 are empirical parameters.

Hence, in this study, we use the BFSAs-wheel to obtain $\sigma(\theta)$ directly from force sensor array and estimate the drawbar pull using Equations (9) and (10). Since c and ϕ are inherent parameters of soil and are constant, so they are identified in advance. We mainly use the motion measurement system using a telecentric optics, which is based on a visual odometry technique, to measure s . k_x is an empirical parameter used to estimate drawbar pull. In this study, we propose a method to estimate k_x from the initial motion of a rover. Thus, the essential parameters for the estimation of F_x are, $\sigma(\theta)$ (determined by the BFSAs wheel), s (determined by using the motion measurement system using a telecentric optics), and k_x (estimated by the initial motion of the rover).

III. DEVELOPMENT OF BFSAs WHEEL

It is very important to accurately measure σ online in order to estimate the drawbar pull of wheels. Therefore, we have developed the BFSAs wheel which can be used to measure σ directly, as described in this section.

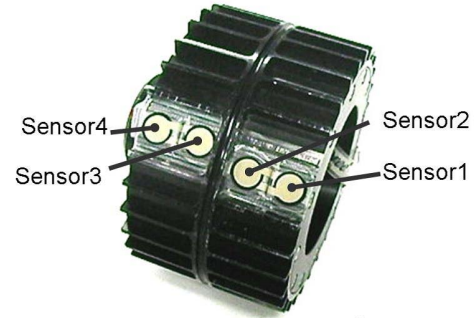


Fig. 3. Built-in force sensor array wheel

A. Structure of BFSAs wheel

The BFSAs-wheel consists of a force sensor array, a microcontroller (H8-3694; Renesas Technology Corp.), and a wireless communication device (ZIG-100B: produced by BestTechnology Co., Ltd.) embedded in a wheel. Four force sensors attached to the surface of the wheel generate a voltage according to the normal stress σ under the wheel. The microcontroller obtains the sensing value via an analog-digital converter. The serial wireless communication device (which consists of a ZigBee module with a frequency of 2.4GHz) is used to communicate with the main controller of the robot. In our experiments, the sampling time is set to 50 ms. For power supply, a small re-chargeable battery is mounted inside the wheel. While the wheel rotates, the main controller of the robot receives a normal stress continuously via the wireless communication to form $\sigma(\theta)$. An image of the BFSAs wheel developed in this study is shown in Fig. 3. The four-sensor array is located across the width of the wheel so that four plots of $\sigma(\theta)$ can be obtained in one rotation of the wheel.

B. Feature of force sensors used in BFSAs wheel

To accurately estimate σ under the wheel, sensors should be as thin as possible. Therefore, we have chosen the FlexiForce button sensors (A201; Nitta Corp.); the thickness and diameter of these sensors are 0.819 mm and 9.5 mm, respectively. The resistance of the sensors is inversely proportional to the force applied. Hence, the sensors can be used to measure forces up to 4.4 N. The sensors have a dead-band up to 0.1 N. However, this band is sufficiently small, and the sensors are suitable for the measurement of $\sigma(\theta)$ in our experiments.

IV. MEASUREMENT OF NORMAL STRESS DISTRIBUTION USING BFSAs WHEEL

We measure $\sigma(\theta)$ using the BFSAs wheel. In this section, the experimental setup and measurement results are described.

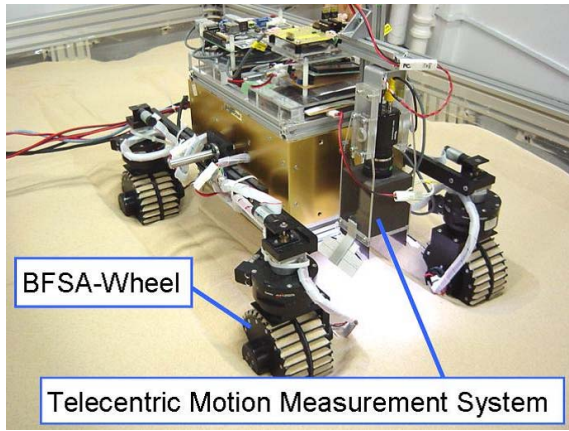


Fig. 4. Overview of rover testbed

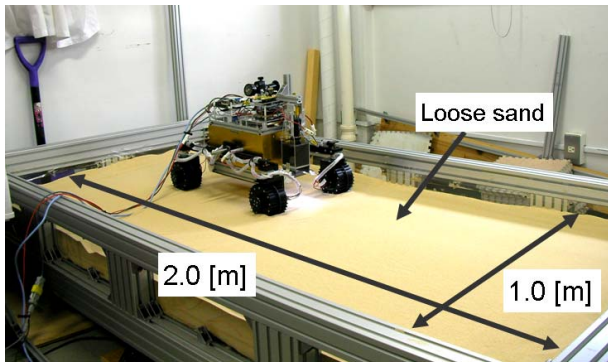


Fig. 5. Overview of the experimental setup

A. Experimental setup

A sandbox, as shown in Fig. 5, with dimensions of 1×2 m is used for the measurement. The sandbox contains a 15 cm thick layer of Toyoura standard sand (JIS R 5201); this sand has very low viscosity and its particle is almost uniform. This implies that $c \approx 0$ in Equation (9). The sandbox can be tilted manually up to 20° ; s of the wheels of the rover can be changed by changing the slope angle α of the sandbox.

The robot used in the study is a four-wheeled rover, shown in Fig. 4, developed in our laboratory. The BFSA wheel is fitted on the front-right of the rover in order to estimate $\sigma(\theta)$ while the rover moves on the target surface. The motion measurement system using a telecentric optics, based on a visual odometry technique, is mounted on the robot body in order to measure the robot velocity without using external devices embedded in the target environment. From the robot velocity and the rotational velocity of the wheel measured by using an encoder, s of each wheel is calculated using Equation (8).

Generally, the velocity of planetary rovers is set to be very low in order to compensate for the time delay in communication. Therefore, in this experiment, we set the rover velocity as 10.4 mm/s, and the inclination of the sandbox is changed from 0° to 8° with an interval of 2° . For the estimation of $\sigma(\theta)$, the rover is made to navigate

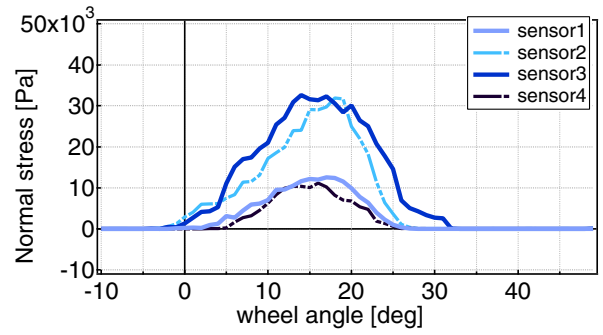


Fig. 6. Experimental normal stress distribution

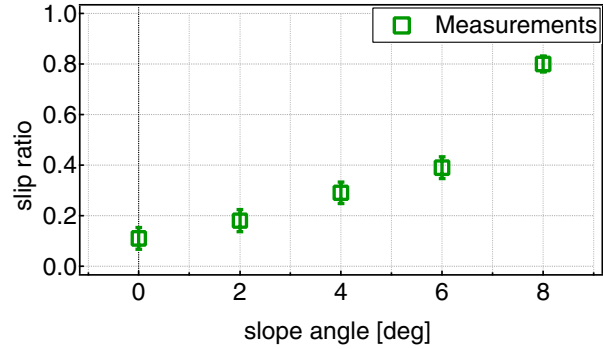


Fig. 7. Slope angle vs. slip ratio

a distance of approximately 1 m. This is repeated three times under each condition. Basically, a slope generates a nonuniform stress between front wheels and rear wheels. However in our case, the slope angle is very small shown in the above, therefore we assume that the slope effect is small enough.

B. Experimental results

Using the BFSA wheel, stable $\sigma(\theta)$ is obtained with high reproducibility. The plots of $\sigma(\theta)$ obtained by using the four sensors are shown in Fig. 6. Each distribution is an average of three measurements. In all the measurement results, the sensing value of sensor 2 is larger than that of sensor 1, and the sensing value of sensor 3 is larger than that of sensor 4. This implies that $\sigma(\theta)$ along the width of the wheel is not uniform and σ mainly acts at the central part of the wheel. In order to simplify the following discussions, we assume that $\sigma(\theta)$ for the following calculation is estimated by an average of four plots of $\sigma(\theta)$ obtained by the four sensors.

Fig.7 shows the plot of α v.s. s . Fig. 8 shows the relationship between the s and $\sigma(\theta)$. It is observed that the peak of $\sigma(\theta)$ shifts forward with increasing s . We consider that the phenomenon is generated by scooping out the soil by a wheel rotation with high slip ratio. It causes increasing a sinkage of the wheel, and the contact part is shifted forward. Further, it has been confirmed that the effective area of $\sigma(\theta)$ on the wheel is considerably smaller (30° on an average) than the actual contact area (70° on an average).

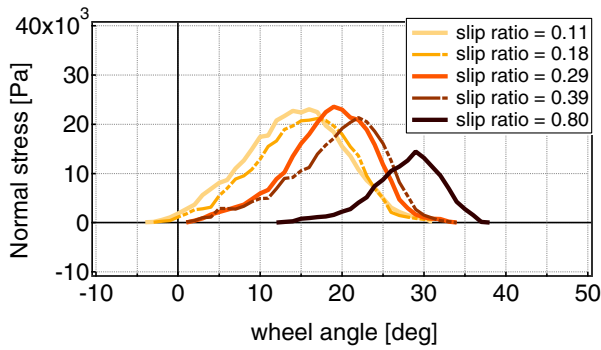


Fig. 8. Comparison of Normal stress distribution

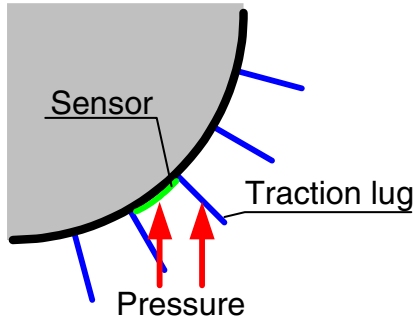


Fig. 9. Relationship among traction lugs, wheel, and pressure from soil

V. ESTIMATION OF SOIL PARAMETERS

From the discussion presented in Section II-D, it is found that the estimation of $\sigma(\theta)$, s , and k_x is very important for estimation of F_x . We have obtained stable $\sigma(\theta)$. s is measured by using the motion measurement system using a telecentric optics. Now, the parameter that has to be estimated is k_x , which is generally difficult to estimate. In this section, we propose an estimation method for k_x on the basis of the above-mentioned experimental results.

A. Definition of magnification coefficient M

Theoretically, the wheel load should be equal to the integral value of σ in the contact area. However, practically, because of the traction lugs on the wheel, which are meant for better grip on the ground, the integral value of σ measured by BFS A wheel is smaller than the wheel load. That is because the traction lugs support the wheel and the effectiveness increases in the front contact area. A schematic of the relationship among the traction lugs, the wheel, and the pressure from soil is shown in Fig. 9. The phenomenon is confirmed by Fig. 8, qualitatively.

In this study, we assume that a measured σ is different from the actual σ , but the shapes of measured $\sigma(\theta)$ almost similar to that of actual $\sigma(\theta)$. Therefore, we introduce a magnification coefficient M to estimate the actual value of σ . It is assumed that the sinkage of the wheel changes according to s of the wheel. Therefore M should change in s .

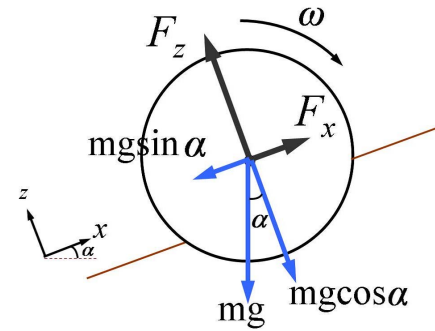


Fig. 10. Drawbar pull and vertical force acting on wheel rotating along slope

B. Estimation of parameters k_x and M

F_x and F_z given by Equations (1) and (2), respectively, can be rewritten as follows:

$$F_x = rb \int_{\theta_r}^{\theta_f} \{\tau_x(\theta) \cos \theta - M\sigma_s(\theta) \sin \theta\} d\theta, \quad (11)$$

$$F_z = rb \int_{\theta_r}^{\theta_f} \{\tau_x(\theta) \sin \theta + M\sigma_s(\theta) \cos \theta\} d\theta, \quad (12)$$

where $\sigma_s(\theta)$ denotes the measured normal stress distribution. $\tau_x(\theta)$ given by Equation (9) can be written as

$$\tau_x(\theta) = (c + M\sigma_s(\theta) \tan \phi) [1 - e^{-j_x(\theta)/k_x}]. \quad (13)$$

The equilibrium force acting on each wheel of the rover when it traverses along a slope angle of α , as shown in Fig. 10, is given by the following equations:

$$F_x = mg \sin \alpha, \quad (14)$$

$$F_z = mg \cos \alpha. \quad (15)$$

k_x and M satisfying the simultaneous equations (11), (12), (14), and (15) are obtained by repetitively using the bisection algorithm.

TABLE I
ESTIMATED k_x

s	k_x [m]
0.11	0.0072
0.18	0.0073
0.29	0.0070
0.39	0.0066
0.80	0.0026

TABLE II
WHEEL-SOIL INTERACTION PARAMETERS AND VALUES

Parameter	Value	Description[unit]
r	0.055	wheel radius [m]
b	0.064	wheel width [m]
mg	28.92	wheel weight [N]
c	0	cohesion stress [kPa]
ϕ	38.0	friction angle [°]

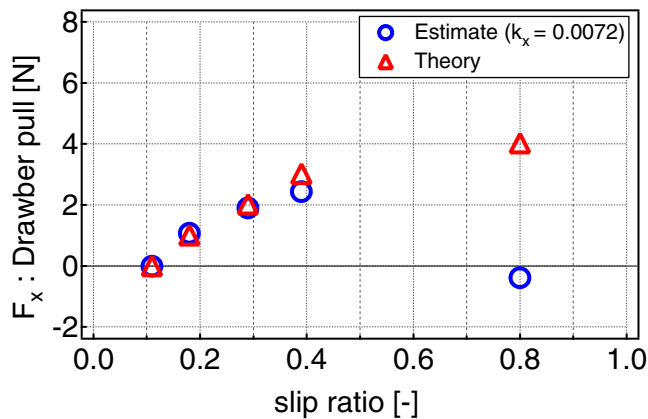


Fig. 11. Comparison of estimated and theoretical values of drawbar pull

C. Estimation of k_x

The soil parameter k_x estimated using the above-mentioned method for different values of s is listed in Table I. The values of other soil parameters are listed in Table II. It is found that k_x remains almost constant except at large values of s . s is found to be large when the wheel is almost half buried in the soil, and the physical interaction between the soil and the wheel in this case appears to be different from that in other cases. Moreover, practically, rovers should not be operated at a very large s in order to prevent their wheels from getting stuck in soil. Therefore, we conclude that the estimated k_x is constant and useful in a low slip ratio area (less than 0.5).

VI. ESTIMATION OF DRAWBAR PULL

When $\alpha = 0$, F_x is assumed to be equal to 0. This implies that the soil parameter k_x can be estimated using the above-mentioned method when the robot traverses a flat terrain. In our case, $k_x = 0.0072$. Then, we calculate F_x for different values of α using the (A) estimated parameters, (B) measured $\sigma(\theta)$, and (C) estimated M . Fig. 11 shows the estimated F_x for s up to 0.5. This implies that a rover that can measure $\sigma(\theta)$ can accurately estimate F_x for s up to 0.5.

VII. CONCLUSIONS AND FUTURE STUDIES

In this paper, a conventional method based on terramechanics, which can be used for the estimation of drawbar pull, and the disadvantages of this method were discussed. Then, a measurement method for normal stress distribution using the BFS wheel was presented, and some experiments based on this method were reported. Finally, our proposed method for the estimation of drawbar pull was validated by estimating drawbar pull for different slope angles. Thus, we proved that a rover with the BFS wheel can estimate its drawbar pull online in the real environments without using external devices embedded in the environment.

In our experiments, only one type of soil (Toyoura standard sand) was used. In our future studies, we would confirm the validity of the proposed method using different types

of wheels and vertical loads. Furthermore, in this research, we assumed that parameters of c and ϕ are obtained in advance. However, these parameters should be identified in applications in the real world. We will develop a method to estimate these parameters online.

ACKNOWLEDGMENTS

REFERENCES

- [1] Mark Maimone, Yang Cheng, and Larry Matthies. Two years of visual odometry on the mars exploration rovers: Field reports. *Journal of Field Robotics*, 24(3):169–186, 2007.
- [2] M. G. Bekker. *Off-The-Road Locomotion*. Ann Arbor, MI, USA, The University of Michigan Press, 1960.
- [3] M. G. Bekker. *Introduction to Terrain-Vehicle Systems*. Ann Arbor, MI, USA, The University of Michigan Press, 1969.
- [4] J. Y. Wong. *Theory of Ground Vehicles*. John Wiley & Sons, 1978.
- [5] K.lagnemma and S.Dubowsky. *Mobile Robots in Rough Terrain : Estimation, Motion Planning, and Control with Application to Planetary Rovers (Springer Tracts in Advanced Robotics 12)*. Germany, Springer, 2004.
- [6] Genya Ishigami, Akiko Miwa, Keiji Nagatani, and Kazuya Yoshida. Terramechanics-based model for steering maneuver of planetary exploration rovers on loose soil. *Journal of Field Robotics*, 24(3):233–250, 2007.
- [7] I.Shmulevich, D.Ronai, and D.Wolf. A new field single wheel tester. *Journal of Terramechanics*, 3:133–141, 1996.
- [8] K.lagnemma, H.Shibly, and S.Dubowsky. On-line traction parameter estimation for planetary rovers. In *Proceedings of the 2002 IEEE Int. Conf. on Robotics and Automation (ICRA '05)*, pages 3142–3147, Washington, DC, USA, 2002.
- [9] Y.Nohse, K.Hashiguchi, and M.Ueno. A measurement of basic mechanical quantities of off-the-road traveling performance. *Journal of Terramechanics*, 28:371–382, 1991.
- [10] Genya Ishigami, Keiji Nagatani, and Kazuya Yoshida. Slope traversal controls for planetary exploration rover on sandy terrain. *Journal of Field Robotics (to be appeared)*, 2009.
- [11] Z.Janosi and B.Hanamoto. The analytical determination of drawbar pull as a function of slip for tracked vehicle. In *Proc. of 1st Int. Conf. on Terrain-Vehicle Systems*, 1961.
- [12] J.Y.Wong and A.R.Reece. Prediction of rigid wheel preformance based on the analysis of soil-wheel stresses part i, performance of driven rigid wheels. *Journal of Terramechanics*, 4:81–98, 1967.